

## Nitrogen-induced interface defects in Si oxynitride

Eun-Cheol Lee

*Division of Bio-Nano Technology, Kyungwon University, Gyeonggi 461-701, Korea  
and Gachon Bio-Nano Research Institute, Gyeonggi 461-701, Korea*

(Received 25 August 2007; revised manuscript received 12 February 2008; published 10 March 2008)

Based on first-principles density-functional calculations, we propose N-associated defects at Si/SiO<sub>2</sub> interface, which behave as dominant interface states in Si oxynitrides instead of conventional  $P_b$  centers in pure SiO<sub>2</sub>. These defects involve an N interstitial, and their energy levels lie in the broad range, from the midgap to the conduction-band edge of Si, depending on local oxidation status near N, while electrical states from  $P_b$ -type centers are removed by substitutional N atoms. Our results provide a mechanism for degradations related to the interface defects in Si oxynitrides which are used in state-of-the-art metal-oxide-semiconductor devices.

DOI: [10.1103/PhysRevB.77.104108](https://doi.org/10.1103/PhysRevB.77.104108)

PACS number(s): 61.72.-y, 71.55.-i, 73.20.-r, 85.30.-z

Defects at Si/SiO<sub>2</sub> interface have been intensively studied for several decades because they act as an interface charge trap which degrades performances and reliabilities of metal-oxide-semiconductor (MOS) transistors. It is well identified by experiments and theories<sup>1-5</sup> that dominant interface defects, the so-called  $P_b$  centers, are isolated dangling bonds from Si substrate near the interface.

Unfortunately, a further study on the interface traps becomes required, as Si oxynitride (or lightly nitrated oxide) has replaced pure SiO<sub>2</sub> in state-of-the-art MOS transistors that are used in commercial semiconductor devices. The nitridation of SiO<sub>2</sub> is essential for suppressing boron penetration from  $p^+$ -polysilicon electrodes.<sup>6</sup> In addition, it also improves electrical properties such as charge trapping,<sup>7</sup> and theoretical models for this effect have already been given.<sup>8,9</sup> On the other hand, the N incorporation at the interface is known to increase densities of interface traps,<sup>10</sup> causing performance degradations and reliability problems.<sup>11-14</sup>

Recent experiments clearly show that new interface defects are created and act as dominant species in Si oxynitrides instead of  $P_b$  center. Stathis *et al.* showed that the interface states are located near the conduction-band edge of Si with a broad energy distribution, through low-voltage stress-induced leakage current (LV-SILC) measurements, while pure oxide shows negligible interface state generation at the conduction-band edge.<sup>15,16</sup> On the other hand, the defect density at midgap is much larger in SiO<sub>2</sub>, as compared to that in oxynitride.<sup>15,16</sup> Campbell *et al.* also observed a new defect center in oxynitride which is fundamentally different from  $P_{b0}/P_{b1}$  defects,<sup>17</sup> through electron spin resonance measurements. Understanding the N-related interface defects on an atomistic level is very important to modern MOS technology, but these defects are not clearly identified yet.

In this paper, we present an atomic model for N-induced defects at the interface between Si and Si oxynitride based on first-principles density-functional calculations. We find that N interstitials at the interface create defect levels in the Si band gap, which move upward from the midgap to the conduction-band edge, as the interactions with oxygen atoms in SiO<sub>2</sub> matrix are enhanced. On the other hand, the deep defect level caused by a  $P_b$ -like center, i.e., a threefold-coordinated Si, is removed by substitution of an N atom. Our model for N-associated interface defects explains the en-

hanced interface state generation near the conduction-band edge and the reduction of midgap defect density in Si oxynitrides.

First-principles pseudopotential calculations are performed using density-functional theory (DFT) within the generalized gradient approximation.<sup>18</sup> We use ultrasoft pseudopotentials for O, N, and H (Ref. 19) and a norm-conserving pseudopotential for Si.<sup>20</sup> A converged plane wave basis set is generated with energy cutoffs of 30 Ry for wave functions and 180 Ry for charge densities, respectively. To describe Si/SiO<sub>2</sub> interface, we construct the interface with Si crystal and tridymite SiO<sub>2</sub> in a supercell containing 128 atoms, similar to the previous theoretical studies.<sup>21,22</sup> This supercell geometry is a periodic slab structure with seven Si layers for bulk Si and two Si and four O layers for SiO<sub>2</sub>, and the Si dangling bonds at both surfaces are passivated by H atoms. The Si band gap of this interface is found to be 1.05 eV, similar to previous calculations.<sup>21</sup> This value is larger than for usual DFT band gap of bulk Si because of the quantum confinement effect in the slab geometry.<sup>21</sup>

First, we study electronic and atomic structures of an N interstitial ( $N_i$ ) and its complexes with oxygen ions at the interface. When an N interstitial is incorporated deep into the Si layers in our interface model, it is found that a (100)-split-interstitial geometry is the most stable, similar to previous calculations on N in Si.<sup>23,24</sup> A symmetric split-interstitial structure at the interface has difficulty maintaining its stability because of lattice strain near the interface. The optimized structure of the  $N_i$  at the interface is illustrated in Fig. 1(a). This defect also includes a trivalent N and Si atom, similar to the (100) split interstitial, and the threefold Si atom ( $Si_I$ ) protrudes into the SiO<sub>2</sub> side.  $Si_I$  is undercoordinated and, thus, a chemically active atom in the defect, while the valence shell of N is completely filled. Due to the asymmetric structure, the  $Si_I$ - $Si_{III}$  distance (3.15 Å) is longer by 0.52 Å than the  $Si_I$ - $Si_{II}$  distance (2.63 Å). A charge density analysis indicates that no bonding occurs between  $Si_I$  and  $Si_{II}$ , although the distance between them is only longer by 0.3 Å than the Si-Si bond length in crystalline Si. The Si-N bond lengths are found to be 1.73–1.85 Å, and nearest-neighbor Si-Si bonds from N are elongated by 0.08 Å to compensate for lattice strain caused by these short Si-N bonds. If posi-

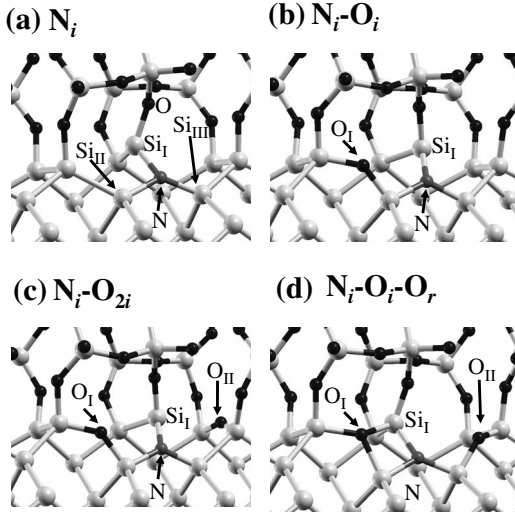


FIG. 1. Atomic structures of the (a)  $N_i$ , (b)  $N_i-O_i$ , (c)  $N_i-O_{2i}$ , and (d)  $N_i-O_i-O_r$  defects at the interface.

tions of the  $Si_I$  and N atom are changed in Fig. 1(a), that geometry would be unrealistic due to the unstable N-O bond, which are not supported by theoretical studies.<sup>25,26</sup> In fact, we investigated a number of geometries of  $N_i$  at other Si sites at the interface for various bonding directions and did not find any significant difference from the structure in Fig. 1(a).

For partially oxidized interface, it is energetically favorable that  $N_i$  forms a complex with O ions. We model partial oxidation of the interface by using O interstitials ( $O_i$ ) incorporated at the Si-Si bonds because our supercell does not include O atoms at the interface, i.e., the top layer of Si. For  $N_i-O_i$  complex, the O interstitial prefers the nearest Si-Si bond sites from the  $N_i$ , as shown in Fig. 1(b); the total energy is lowered by 0.62 eV than for an isolated  $O_i$  at the same Si layer and an isolated  $N_i$  because of a coordinate covalent bonding of  $Si_I$  with the  $O_i$ . Thus, nearest-neighbor Si-Si bonds from N are expected to behave as attracting centers for O ions in partially oxidized interfaces. The  $Si_I$  atom is shifted away by 0.37 Å from its initial position to reduce repulsive Coulomb interaction with the lone-pair orbital of  $O_i$ . When the second O ion ( $O_{II}$ ) is incorporated at another nearest-neighbor bond from N,  $Si_I$  and  $O_I$  atoms become fourfold and threefold coordinated, respectively, by forming the  $Si_I-O_I$  bond [see Fig. 1(d)]. We refer to this structure as  $N_i-O_i-O_r$  complex, where  $O_r$  means a threefold-coordinated O atom. The complex is more stable by 1.04 eV than an isolated  $N_i$  and two isolated  $O_i$ . This structure is similar to that of the  $O_i-O_{2r}$  complex, which is shallow thermal donor in Si,<sup>27,28</sup> if N is replaced by an O atom. The  $N_i-O_{2i}$  structure, in which  $Si_I-O_I$  is broken, is found to be unstable in the same  $O_i$  positions because of lattice strain near the interface, although the similar defect,  $N_i-O_{2i}$  with  $C_{2v}$  symmetry, is suggested to be stable in bulk Si.<sup>23,24</sup> On the other hand, the  $N_i-O_{2i}$  complex becomes stable, when  $O_{II}$  moves to the second-nearest-neighbor Si-Si bond, as shown in Fig. 1(c). This defect is less stable by 0.16 eV than for  $N_i-O_i-O_r$ . We find that an isolated  $O_{II}$  at the first Si layer is more stable by 0.18 eV than an isolated  $O_I$  at the second Si layer. Compared

TABLE I. Single-particle defect levels ( $E_{KS}$ ), defect transition levels ( $E_{-/0}$ ) between neutral and negatively charged states, and Si-O distances for  $N_i$ -related defects.  $E_c$  indicates the conduction-band minimum of Si.

Defect	$E_{KS}$ (eV)	$E_{-/0}$ (eV)	Distance (Å)	
			$Si_I-O_I$	$Si_I-O_{II}$
$N_i$	$E_c-0.4$	$E_c-0.31$		
$N_i-O_i$	$E_c-0.29$	$E_c-0.20$	3.36	
$N_i-O_i-O_r$	$E_c$	$E_c$	1.85	3.33
$N_i-O_{2i}$	$E_c-0.19$	$E_c-0.12$	3.32	3.47

to  $N_i-O_i$  plus an isolated  $O_{II}$ , the binding energy of  $N_i-O_{2i}$  is found to be 0.08 eV. It increases to 0.26 eV, as referenced to an isolated  $O_I$  and  $N_i-O_i$ . The  $Si_I-O_{II}$  distance, 3.47 Å, is not much different from other Si-O distances lying in the range of 3.32–3.36 Å except for the  $Si_I-O_I$  distance of  $N_i-O_i-O_r$  (see Table I). The interaction between  $Si_I$  and  $O_{II}$  is also found in the defect level, shown in Fig. 2(a), where the lone-pair orbital of  $O_{II}$  is hybridized. Because of exothermic binding energies, N interstitials might form complexes with oxygen ions at the interface. The main features found here are expected to be unchanged even for amorphous  $SiO_2$  because the geometries of  $N_i$ -related defects are mainly determined at the silicon side of the interface, as exhibited in Figs. 1(a)–1(d).

Here, we find that energy levels of  $N_i$ -associated interface defects are shifted upward in Si band gap, as interactions with O ions are enhanced. The shifts of defect levels do not result from direct interactions between  $N_i$  and  $O_i$ , but from the interactions of threefold Si atoms created by  $N_i$  with  $O_i$ . To deal with charge capture process via nonequilibrium tunneling process, we analyze the single-particle defect levels of neutrally charged defects. The calculated defect levels for the  $N_i$ -related defects are listed in Table I, as referenced to the bottom of the conduction band ( $E_c$ ). For  $N_i$ , a deep defect level is found at  $E_c-0.4$  eV. The level does not arise from the N atom itself but from the dangling bond of the threefold Si atom, similar to the  $N_i-O_{2i}$  characterized in Fig. 2(a). For  $N_i-O_i$ , the defect level is elevated by 0.11 eV because of the Coulombic repulsion between the lone-pair orbital of  $O_I$  and the dangling bond of  $Si_I$ . Contrary to our results, it is re-

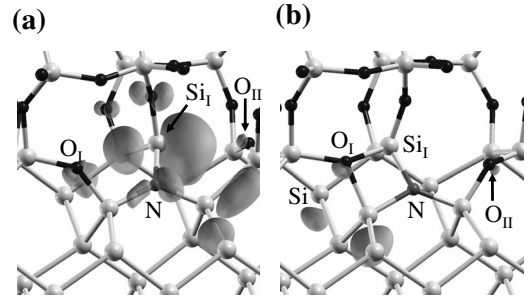


FIG. 2. Charge densities are plotted for the defect levels of the (a)  $N_i-O_{2i}$  and (b)  $N_i-O_i-O_r$  defects for an isosurface of 0.002 a.u.

ported that the defect state becomes deeper for bulk Si after the formation of  $N_i-O_i$  complex;<sup>24</sup> this is attributed to the fact that the dangling bond orbital of  $N_i-O_i$  becomes more localized after the symmetry of the  $N_i$  is broken. For the  $N_i-O_i-O_r$  defect, it is found that a shallow-level interface state near  $E_c$  is created. The physical origin of the shallow interface state can be explained as follows; as shown in Fig. 1(d), this defect contains no undercoordinated Si atom and thereby does not have the defect level associated with the Si dangling bond. Instead, one excess electron is left after filling the valence shell of overcoordinated  $O_i$ , and this electron may be transferred to an antibonding orbital of  $Si_i$  and  $O_i$ . However, since this antibonding orbital [Fig. 2(b)] lies above the conduction band, the electron may occupy the conduction band and thus the creation of the shallow level is expected by the effective mass theory. The key component of the shallow-level defect is the threefold-coordinated oxygen atom. If  $O_i$  in  $N_i-O_i-O_r$  is replaced by a N atom, the defect has no undercoordinated or overcoordinated atoms; the Si, N, and O atoms are fourfold, threefold, and twofold coordinated, respectively. Thus, this defect might be an electrically inactive complex with no defect levels in the Si band gap. Although the chemical structure of  $N_i-O_i-O_r$  is almost identical to that of this inactive defect, the threefold O atom ( $O_r$ ) has one more electron than the N atom. Since  $N_i-O_i-O_r$  has no defect levels in the band gap, it is expected that the shallow level just below the conduction band is created, similar to the phosphorus defect in Si. Other interface defects involving a stable threefold O atom might also have shallow defect levels near the conduction band. For the  $N_i-O_{2i}$  complex, the defect level moves down to 0.19 eV below the conduction-band minimum, as the bond of the  $Si_i$  and the  $O_{II}$  atoms is broken. However, it is still affected by  $O_{II}$ , as discussed earlier, and thereby higher by 0.1 eV than for  $N_i-O_i$ . We also analyze thermodynamic defect transition levels, which are obtained from the energy difference of two relaxed geometries with different charges. The transition levels between neutral and negative charge states are calculated because these levels describe the electron tunneling from interface traps below the  $n$ -well Fermi level into the  $p^+$ -polysilicon electrode, which leads to the LV-SILC in  $p$ -type metal-oxide-semiconductor field-effect transistor.<sup>15</sup> As listed in Table I, the calculated transition levels are pushed upward from  $E_c-0.31$  eV to  $E_c$ , as the interaction with O ion is enhanced, similar to the single-particle levels. Thus, our results show that energy levels of  $N_i$ -related defects possibly lie in the broad energy range from the midgap to conduction-band edge, depending on the degree of interactions with O ions. For amorphous  $SiO_2$ , more broad level distributions are expected because of more various local configurations of oxygen atoms.

On the other hand, we find that a substitutional N atom possibly removes electrical activity of an interfacial Si dangling bond, the so-called  $P_b$  center, as reported in previous theoretical calculations,<sup>29</sup> although the  $N_i$ -related species act as an interface trap. In our previous calculations, we suggest that most of the substitutional N atoms ( $N_{Si}$ ) exist as an N pair at interface, while single N is unstable due to the creation of a dangling bond.<sup>8</sup> However, single substitutional N is stabilized, when it replaces a threefold-coordinated Si with

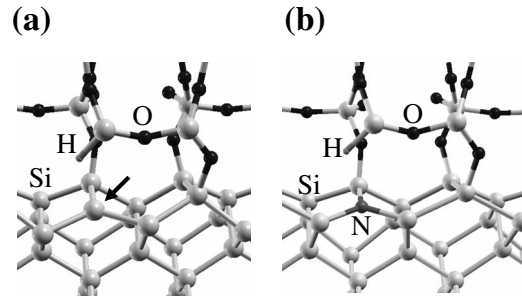


FIG. 3. Atomic models of the (a)  $P_b$  center and (b)  $N_{Si}$  at the interface. The arrow in the figure indicates a threefold-coordinated Si.

an unpaired dangling bond. To validate this argument, we first construct a model geometry for  $P_b$  center as in Fig. 3(a). This model is similar to the dimer model for the  $P_{b1}$  defect in the previous calculations,<sup>5</sup> but our conclusions are not affected even if other interface models are used. We find that undercoordinated Si is possibly replaced by a threefold N atom without any remaining dangling bond orbital, as shown in the  $N_{Si}$  defect [see Fig. 3(b)]. This defect is an electrically inactive center with no defect level in the band gap, while a deep level is found at  $E_c-0.4$  eV for our  $P_b$  center model. We investigate the stability of  $N_{Si}$  defect via the reaction,  $P_b$  center +  $N_i$  (at the interface)  $\rightarrow$   $N_{Si}$  (at the interface) + Si (of perfect crystal), and find that this reaction is exothermic by 1.93 eV. Thus, the annihilation of the  $P_b$  center by substitution of N is energetically favorable in Si oxynitride.

The experimentally reported interface states and suppressed  $P_b$  centers in Si oxynitrides are explained by our proposed models for N-interstitial-related and substitutional N defects, respectively. In LV-SILC and gated diode measurements, the interface states in oxynitrides are found to be distributed over a broad energy range in the upper portion of the Si band gap.<sup>15</sup> We showed that the defect levels for the  $N_i$ -related species are possibly located at various positions between the midgap and the conduction-band edge, depending on interactions with neighboring O atoms, in good agreement with the experiments. Among the defects distributed over the broad range, it is expected that the concentrations of conduction-band edge defects such as  $N_i-O_i-O_r$  are higher than for midgap defects due to the following reasons. The isolated N interstitial produces a deep interface state, but it is only stabilized at the oxygen-free interface like Fig. 1(a), where the top layer of Si bears no oxygen atom. For a partially oxidized interface, which is usually expected in normal oxidation process,  $N_i$  might attract O atoms because of the exothermic binding energies, and thus the defect levels are pushed upward by the interactions with O atoms. Especially, defects involving trivalent O atoms might greatly enhance LV-SILC, since they possess defect levels close to the conduction band. The suppression of midgap states<sup>16</sup> is explained by the removal of  $P_b$ -center-like defect by substitutional N atoms. However, electrical improvement of the interface is not guaranteed by the removal of  $P_b$  centers, since the  $N_i$ -associated species possibly degrade interface properties. Our N-defect models only involve  $N \equiv Si_3$  species, i.e., one N bonded to three Si atoms, in good agreement



with x-ray photoelectron spectroscopy measurements for interfacial N atoms, while the chemical bond of N away from the interface is possibly to be either N bonded to two Si and one O atom (O-N=Si<sub>2</sub>) or N bonded to two Si atoms (N=Si<sub>2</sub>).<sup>25,26,30-33</sup> Thus, our calculations successfully explain the recent experiments for the N-related species in ultrathin Si oxynitrides which have not been fully understood.

In conclusion, we investigate the N-induced defects at the Si/SiO<sub>2</sub> interface through *ab initio* pseudopotential calculations. We find that the N interstitials at the interface create various defect levels in the Si band gap, which range from the midgap to the conduction band of Si. The level positions

are dependent on the configuration of oxygen atoms around the N interstitial. On the other hand, the midgap level caused by  $P_b$  center is possibly removed by substitution of an N atom for a threefold-coordinated Si atom in the defect. Our calculations explain why the interface state generation is enhanced in Si oxynitride, especially near the conduction-band edge of Si, although the density of  $P_b$  center is reduced.

This work was supported by the Kyungwon University Research Fund in 2007. Calculations in this work have been done using the QUANTUM-ESPRESSO package,<sup>34</sup> and all figures were generated by XCRYSDEN program.<sup>35</sup>

- 
- <sup>1</sup>P. Caplan, E. Poindexter, B. Deal, and R. Razouk, *J. Appl. Phys.* **50**, 5847 (1979).
- <sup>2</sup>F. C. Rong, J. F. Harvey, E. H. Poindexter, and G. J. Gerardi, *Appl. Phys. Lett.* **63**, 920 (1993).
- <sup>3</sup>H. J. von Bardeleben, M. Schoisswohl, and J. L. Cantin, *Colloids Surf., A* **115**, 277 (1996).
- <sup>4</sup>A. Stesmans and V. V. Afanas'ev, *J. Appl. Phys.* **83**, 2449 (1998).
- <sup>5</sup>A. Stirling, A. Pasquarello, J.-C. Charlier, and R. Car, *Phys. Rev. Lett.* **85**, 2773 (2000).
- <sup>6</sup>D. Mathiot, A. Straboni, E. Andre, and P. Debenest, *J. Appl. Phys.* **73**, 8215 (1993).
- <sup>7</sup>D. Misra, *Appl. Phys. Lett.* **75**, 2283 (1999).
- <sup>8</sup>E.-C. Lee and K. J. Chang, *Phys. Rev. B* **66**, 233205 (2002).
- <sup>9</sup>S. Jeong and A. Oshiyama, *Phys. Rev. Lett.* **86**, 3574 (2001).
- <sup>10</sup>C. H. Ang, S. S. Tan, C. M. Lek, W. Lin, Z. J. Zheng, T. Chen, and B. J. Cho, *Electrochem. Solid-State Lett.* **5**, G26 (2002).
- <sup>11</sup>H.-H. Tseng, Y. Jeon, P. Abramowitz, T.-Y. Luo, L. Herbert, J. J. Lee, J. Jiang, P. J. Tobin, G. C. F. Yeap, M. Moosa *et al.*, *IEEE Electron Device Lett.* **23**, 704 (2002).
- <sup>12</sup>J. Ushio, T. Maruizumi, and K. Kushida-Abdelghafar, *Appl. Phys. Lett.* **81**, 1818 (2002).
- <sup>13</sup>S. S. Tan, T. P. Chen, J. M. Soon, K. P. Loh, C. H. Ang, and L. Chang, *Appl. Phys. Lett.* **82**, 1881 (2003).
- <sup>14</sup>S. Fujieda, Y. Miura, M. Saitoh, E. Hasegawa, S. Koyama, and K. Ando, *Appl. Phys. Lett.* **82**, 3677 (2003).
- <sup>15</sup>J. H. Stathis, G. LaRosa, and A. Chou, *Proceedings of the International Reliability Symposium* (IEEE, Piscataway, 2004), p. 1.
- <sup>16</sup>J. H. Stathis, R. Bolam, M. Yang, T. B. Hook, A. Chou, and G. Larosa, *Microelectron. Eng.* **80**, 126 (2005).
- <sup>17</sup>J. P. Campbell, P. M. Lenahan, A. T. Krishnan, and S. Krishnan, *Proceedings of the International Reliability Physics Symposium* (IEEE, Piscataway, 2006), p. 442.
- <sup>18</sup>J. P. Perdew, K. Burke, and M. Ernzerhof, *Phys. Rev. Lett.* **77**, 3865 (1996).
- <sup>19</sup>D. Vanderbilt, *Phys. Rev. B* **41**, 7892 (1990).
- <sup>20</sup>A. M. Rappe, K. M. Rabe, E. Kaxiras, and J. D. Joannopoulos, *Phys. Rev. B* **41**, 1227 (1990).
- <sup>21</sup>T. Yamasaki, C. Kaneta, T. Uchiyama, T. Uda, and K. Terakura, *Phys. Rev. B* **63**, 115314 (2001).
- <sup>22</sup>Y.-S. Kim and K. J. Chang, *Appl. Phys. Lett.* **87**, 041903 (2005).
- <sup>23</sup>D. J. Chadi, *Phys. Rev. Lett.* **77**, 861 (1996).
- <sup>24</sup>C. P. Ewels, R. Jones, S. Öberg, J. Miro, and P. Deák, *Phys. Rev. Lett.* **77**, 865 (1996).
- <sup>25</sup>G.-M. Rignanese, A. Pasquarello, J.-C. Charlier, X. Gonze, and R. Car, *Phys. Rev. Lett.* **79**, 5174 (1997).
- <sup>26</sup>G. F. Cerofolini, A. P. Caricato, L. Meda, N. Re, and A. Sgamellotti, *Phys. Rev. B* **61**, 14157 (2000).
- <sup>27</sup>M. Ramamoorthy and S. T. Pantelides, *Appl. Phys. Lett.* **75**, 115 (1999).
- <sup>28</sup>M. Pesola, Y. J. Lee, J. von Boehm, M. Kaukonen, and R. M. Nieminen, *Phys. Rev. Lett.* **84**, 5343 (2000).
- <sup>29</sup>T. Yamasaki and C. Kanata, in *Silicon Nitride and Silicon Dioxide Thin Insulating Films*, edited by R. E. Sah, K. B. Sundaram, M. J. Deen, D. Landeer, W. D. Brown, and D. Misra, (ECS, Pennington, 2003), p. 308.
- <sup>30</sup>D. Bouvet, P. A. Clivaz, M. Dutoit, C. Coluzza, J. Almeida, and G. Margaritondo, *J. Appl. Phys.* **79**, 7114 (1996).
- <sup>31</sup>Z. H. Lu, S. P. Tay, R. Cao, and P. Pianetta, *Appl. Phys. Lett.* **67**, 2836 (1995).
- <sup>32</sup>E. C. Carr, K. A. Ellis, and R. A. Buhrman, *Appl. Phys. Lett.* **66**, 1492 (1995).
- <sup>33</sup>Y. Miura, H. Ono, and K. Ando, *Appl. Phys. Lett.* **77**, 220 (2000).
- <sup>34</sup>S. Baroni, A. D. Corso, S. de Gironcoli, P. Giannozzi, C. Cavazzoni, G. Ballabio, S. Scandolo, G. Chiarotti, P. Focher, A. Pasquarello *et al.*, <http://www.pwscf.org/>
- <sup>35</sup>A. Kokalj, *Comput. Mater. Sci.* **28**, 155 (2003).